

Improved activation and hydrogen storage properties of an amorphous $\text{Mg}_{85}\text{Ni}_{15}$ melt-spun alloy via surface treatment with NH_4^+ solution

Eric A. Lass

*Metallurgy Division
National Institute of Standards and Technology
Gaithersburg, MD USA*

Tel: 301-975-2080; Fax: 301-975-8699;

Email: eric.lass@nist.gov

Abstract

An amorphous $\text{Mg}_{85}\text{Ni}_{15}$ melt-spun hydrogen storage alloy, processed by submersion in an aqueous solution of NH_4^+ , is able to absorb >5 wt. % hydrogen at 473 K during the first hydrogenation cycle. The nanocrystalline microstructure formed during devitrification of the metallic glass is preserved by the lower required activation temperature of the NH_4^+ -treated material; and the kinetics of subsequent absorption/desorption cycles at 573 K are dramatically improved, compared to the as-spun material. DSC experiments and thermodynamic calculations demonstrate that the decreased crystallite size of the 473 K activated material lowers the hydride decomposition temperature by 20 K to 50 K, in contrast to a sample activated at 573 K. The NH_4^+ -treatment of a glassy alloy presented here provides a more practical approach to both forming a nanocrystalline material, and facilitating activation, compared to ball milling; requiring much less time and a more commercially scalable option.

1. Introduction

Mg-based alloys are of great interest to the area of hydrogen storage because of their high gravimetric capacity, low density, and low cost. They suffer from significant drawbacks, however. Among these, is the tendency of Mg to oxidize, forming a passivating layer of MgO ,

significantly reducing the kinetics of the hydriding reaction [1-3]. Activation, usually by exposure to hydrogen at elevated temperatures in excess of 573 K, is therefore necessary to break up or remove this surface layer. Ball milling (BM) or mechanical alloying (MA) is often utilized, and serve two purposes. First, BM and MA break up the material, exposing fresh, unoxidized surface, which facilitates the activation process. Processing via BM and MA also create nanostructured materials. Hydrogen absorption/desorption kinetics are significantly improved by the increases surface area to volume ration of the powders, compare to bulk materials. Additionally, capillarity, or the Gibbs-Thomson effect can theoretically alter the thermodynamics of the hydriding process when grain/particle size becomes small enough.

These processes are time consuming, however, sometimes taking several tens to hundreds of hours. And if the BM material is exposed to air, a surface oxide will reform, compromising the advantage of improved activation. Additionally, when activated at temperatures of 573 K or greater, more than 0.6 of the melting temperature of Mg, the nanocrystalline nature of the material is destroyed by microstructural coarsening occurs.

Because of the limitations of the above processes, it is advantageous to develop new methods creating nanocrystalline structures, and activating them without exposure to such elevated temperatures. In the present work, an aqueous solution of NH_4^+ is used to treat the surface of an Mg-based melt-spun metallic glass prior to activation, dissolving the passivating MgO. The resulting material demonstrates improved activation and hydrogen storage properties, compared to the as-spun alloy.

2. Experimental

Appropriate amounts of 99+ % pure Mg and 99.9 % pure Ni were measured to produce a 50 g sample with a nominal composition of (in at. %) $\text{Mg}_{85}\text{Ni}_{15}$. Compositional analysis of preliminary melting trials, an additional 10 wt. % Mg was added to the alloy prior to melting to accommodate for the loss of Mg vapor. The material was induction melted in an Ar atmosphere and cast into a cooled Cu mold. The composition of the ingot was measured using energy dispersive x-ray spectroscopy (EDS), and was found to be within 0.5 at. % of the target composition. The surface of the as-cast ingot was removed to reduce any contamination. The ingot was then cut into pieces for melt spinning (MS). MS was performed under a He environment by ejecting a small amount (1 to 2 g) of melted alloy onto a 20 cm diameter Cu wheel spinning at a speed of 3000 RPM.

A portion of the ribbons were treated by submersion in an agitated aqueous solution of 30 % (by mass) ammonia for two minutes. The ribbons were then immediately rinsed in a bath of hexanes, and allowed to dry in air. Hexanes have been reported to prevent oxidation of Mg after processing when used during ball milling of Mg-based alloys [4]. After exposure to aqueous NH_4^+ , the treated ribbons looked no different than in the as-spun condition. A second portion of the MS ribbons were ball milled (BM) in hexanes with a ball to sample mass ratio of 20:1 for 30 min to physically break up the surface oxide, providing fresh unoxidized surfaces. The powder was recovered from the hexanes and allowed to dry in air. Still another portion of the MS ribbon was left untreated as a control, and will be referred to as in the as-spun condition.

Hydrogen absorption kinetics measurements were performed using a Sieverts-type apparatus under a H_2 pressure of 2 MPa at temperatures of 473 K and 573 K. Desorption kinetics were measured at a pressure of less than 3 kPa. The activation cycle, considered the first

hydriding cycle, was carried out at 473 K or 573 K, while all subsequent cycles were performed at 573 K. To ensure complete activation of an entire sample, hydriding kinetics were measured using the third absorption/desorption cycle.

A portion of the ribbons were heat-treated in an inert atmosphere at temperatures of 473 K and 573 K to study devitrification and microstructural coarsening. Structural characterization of as-spun, heat treated, and hydrided materials was performed using x-ray diffraction (XRD). An Al₂O₃ standard was used to measure the instrument peak broadening for calculating average crystallite size. Hydride decomposition temperatures were also measured using differential scanning calorimetry (DSC) under an Ar environment.

3. Results and discussion

3.1. Devitrification of the melt-spun ribbons

Figure 1 shows the XRD patterns for the MS Mg₈₅Ni₁₅ ribbon as-spun, heat treated at 473 K and 573 K for 5 min, and at 473 K for 1 week. In the as-spun condition, the material is x-ray amorphous, indicated by the broad amorphous “hump,” and lack of any observable crystalline peaks. At 473 K, the first phase observed to crystallize from the amorphous phase is the metastable Mg₆Ni intermetallic, isomorphous with Mg₆Pd. When the sample is heat treated at 573 K for 5 min, this phase immediately begins to decompose into the equilibrium two-phase microstructure of HCP Mg and Mg₂Ni intermetallic. After 1 week at 473 K, decomposition of Mg₆Ni into the equilibrium phases is also observed; however a small amount of the metastable phase is still present. These results are in agreement with previous reports of crystallization in alloys of similar composition [5].

Comparison of the XRD pattern of the ribbons heat treated at 573 K for 5 min and 473 K for 1 week in Figure 1 demonstrates much increased kinetics at 573 K compared to 473 K. Peak widths in the two scans are similar. From a Reitveld refinement of the two patterns, using only the non-overlapping HCP Mg and Mg₂Ni peaks, the average crystallite size of the samples are estimated to be 102±72 nm and 104±35 nm for the samples heat treated at 573 K for 5 min and at 473 K for 1 week, respectively. If both grain sizes are considered equal, LSW can be used to compare the coarsening rate at the two temperatures, $K_{573\text{ K}} t_{573\text{ K}} = K_{473\text{ K}} t_{473\text{ K}}$. Microstructural coarsening at 573 K is found to be three orders of magnitude faster than at 473 K, $K_{573\text{ K}}/K_{473\text{ K}} \approx 2000$.

3.2. Activation cycle

Figure 2 shows the first absorption cycle (activation) of the MS ribbons in all three conditions, ball milled, NH₄⁺ treated, and as-spun, at temperatures of 573 K (Figure 2a) and 473 K (Figure 2b). Ball milling and NH₄⁺-treatment both dramatically improve the kinetics of the activation process. At 573 K, the BM sample absorbs nearly 4.9 wt. % H after 800 min; absorbing roughly 4 wt. % after only 200 min. The NH₄⁺-treated sample exhibits similar behavior to the ball milled material at 573 K, although the kinetics are slightly slower. After absorbing about 4 wt. % H after 300 min, the hydriding kinetics slow, and after 800 min the amount of absorbed H is 4.4 wt. %. In contrast, the as-spun sample reaches only 3.5 wt. % H in 800 min; only 64 % of the 5.5 wt. % theoretical capacity of the alloy, calculated from the equilibrium phase fractions of 0.55 mol HCP Mg and 0.15 mol Mg₂Ni. The rapid initial absorption kinetics at 573 K of the ball milled sample compared to the NH₄⁺ treated one is expected because of the increased exposed surface area of a powder, compared to a ribbon.

Figure 2b demonstrates that BM and NH_4^+ treated ribbons can be activated at a temperature of 473 K, while the as-spun material could not absorb more than 0.25 wt. % H at this temperature. In fact, the activation process for both the BM and NH_4^+ treated samples at 473 K is faster than the as-spun material at 573 K. The NH_4^+ treated ribbon is seen to initially absorb H more rapidly than the BM powder during activation at 473 K. This reason for this observation is not intuitively obvious. Because of the short length of ball milling time, compared to many hours used in other H-storage studies of ball-milled Mg-base materials [1], the average particle size of the ball-milled sample is on the order of 25 μm , the same length scale as the thickness of the melt spun ribbons (10 μm to 30 μm). Moreover, a decrease in particle size would tend to increase, not decrease kinetics, due to the larger surface area to volume ratio. Thus, it is not the likely answer. Grain size refinement during ball milling is also not relevant because of the amorphous nature of the starting ribbon material. However, ball milling, even for short periods of time, is likely to result in compressive stresses and strains in the material, concentrated near surfaces. The hydriding process of pure Mg results in a volume expansion of 30 % when the hydride is formed. It is possible that residual compressive stresses introduced by ball milling act as an additional activation barrier for nucleation of MgH_2 in the Mg particles. At 573 K, the driving force for hydride formation and available thermal energy is large enough to overcome the strain-energy induced activation barrier observable change in kinetics. At 473 K however, the available thermal energy is not enough to readily overcome the additional energy barrier, resulting in slower kinetics during the initial stages of activation. Once the hydride has formed in the stressed surface material, hydriding proceeds exactly as a material that was not exposed to the ball milling process.

All three samples in Figure 2a exhibit a two-stage activation process at 573 K, evidenced by the *s*-shaped curves. This behavior is also observed to lesser extent during activation at 473 K. The reason for this phenomenon is unclear, and is out of the scope of the present work. Because it is observed only during the first hydriding cycle, and has not been reported in hydriding studies of other Mg-based materials with similar compositions, it could be due to initial devitrification of the metallic glass into the metastable Mg₆Ni phase.

3.3. Kinetics of activated material

In Figure 3, the third cycle absorption and desorption characteristics for samples in the three conditions are shown. The third cycle is chosen to ensure that the samples are fully activated by the first two cycles. The kinetics of the as-spun ribbon are much slower than either of the two treated samples. On absorption, the as-spun material absorbs 4.2 wt. % H after 200 min. Absorption is very slow thereafter, reaching only 4.6 wt. % H after 800 min. Desorption in the as-spun ribbon is more rapid than absorption, but still much slower than desorption in the treated samples, requiring 100 min to fully desorb 4.6 wt. % H. Table 1 summarizes the maximum capacities, as well as the times required to reach full and half of the maximum capacities during absorption and desorption.

The ball milled and NH₄⁺-treated samples both exhibit much improved kinetics compared to the as-spun material. From Figure 3 and the absorption/desorption times given in Table 1, treatment with NH₄⁺ results in kinetics very similar to those produced via ball milling. The primary reason behind this result is the decreased exposure time at 573 K. The as-spun sample was activated over night at 573 K, while the ball milled and NH₄⁺-treated samples were held at 473 K over night during activation. Decreased exposure time at 573 K, mitigates microstructural

coarsening, and preserves the nanocrystalline structure of the devitrified ribbons. This has the effect of maintaining shorter diffusion distances for H to travel to reach the Mg and Mg₂Ni, improving the overall kinetics of the hydriding reaction. Because the binary alloy studied here requires temperatures greater than 473 K for reversible hydrogen storage, microstructural coarsening will still occur at operating temperature. However, other Mg-based alloys and composite materials, exhibited reversible H-storage at lower temperatures, will benefit from the ability to activate the material below 573 K.

3.4. Thermodynamic implications

In addition to improving kinetics, decreasing grain/particle size into the nanometer range can theoretically change the thermodynamics of the hydriding reaction because of large surface area to volume ratios and interfacial/surface contributions to the free energy. By decreasing the temperature required to hydride a Mg-alloy, the nanocrystalline structure, created here by the devitrification of the glassy phase, can be preserved for a longer periods of time because of decreased microstructural coarsening kinetics. Figure 4a shows the XRD patterns for the NH₄⁺ treated material which has undergone a single hydrogen absorption cycle at temperatures of 473 K and 573 K. There is evidence of some Mg₂Ni and Mg₆Ni phases left in the patterns due to incomplete hydriding of the samples. The predominant phases in both are MgH₂ and Mg₂NiH₄, as expected for the hydrided alloy. From the relative intensities of the peaks corresponding to each phase, the phase fractions of the two hydrides are similar in both cases. The peaks are broader for the sample hydrided at 473 K, compared to those of the 573 K hydrided material, suggesting a smaller average crystallite size. From a Reitveld refinement of the XRD data in Figure 4a, using only the non-overlapping MgH₂ peaks, the average crystallite size of the MgH₂,

given in Table 2, are 38 ± 9 nm and 58 ± 15 nm, for the samples hydrided at 473 K and 573 K, respectively.

In Figure 4b, DSC scans of the materials hydrided at 473 K and 573 K are shown. The small peak just above 500 K in the 573 K hydrided material corresponds to a polymorphic phase transformation in Mg_2NiH_4 from the low temperature monoclinic structure to the high temperature cubic one. From Figure 4b, extrapolation of the exothermic dehydriding peak in the 473 K hydrided sample yields an onset temperature of 524 K. The onset of dehydrogenation in the material hydrided at 573 K, in contrast, is 573 K. The decrease in the onset of dehydrogenation can be attributed to the decrease in average crystallite size of the hydrides.

If the surface energy of the nonhydride phase in an H_2 atmosphere is greater than that of the hydride, the excess energy will be released when the materials is hydrogenated, effectively reducing the enthalpy of formation of the hydride, ΔH_f . These effects will become important only when the grain/particle size is reduced to the nanometer range. If the surface energies of the two solid phases are considered, equilibrium occurs when the free energy of the hydride phase plus its surface energy is equal to the free energy of the dehydrided phase plus its surface energy, plus the free energy of the hydrogen gas. For $\text{Mg} + \text{H}_2 \rightarrow \text{MgH}_2$, the equation for equilibrium is

$$G_{\text{MgH}_2}^o + A_S^{\text{MgH}_2} \gamma_{\text{MgH}_2} - \left(V_{\text{Mg}} G_{\text{Mg}}^o + A_S^{\text{Mg}} \gamma_{\text{Mg}} + G_{\text{H}_2}^o \right) = 0 \quad (1)$$

where G_Φ^o is the free energy of the phase Φ disregarding surface effects, which depends on both temperature and pressure. V_Φ is the molar volume of phase Φ ; and A_Φ^S and γ_Φ are the surface area and surface energy of phase Φ , respectively. For a spherical particle of radius r , the surface area to volume ratio is

$$\frac{4\pi r^2}{\left(\frac{4\pi r^3}{3}\right)} = \frac{3}{r} \quad (2)$$

If the molar volumes of Mg and MgH₂ are assumed to be equal, substitution of $(3\bar{V})/r$ into Eq. (1), and rearranging yields the equation for equilibrium of Mg and MgH₂ particles of radius r ,

$$\bar{G}_{\text{MgH}_2}^o - (\bar{G}_{\text{Mg}}^o + \bar{G}_{\text{H}_2}^o) + \frac{3\bar{V}}{r} \Delta\gamma_{\text{Mg} \rightarrow \text{MgH}_2} = 0 \quad (3)$$

where \bar{G}_{Φ}^o is the molar free energy of phase Φ , \bar{V} is molar volume, and $\Delta\gamma_{\text{Mg} \rightarrow \text{MgH}_2}$ is the difference in surface energies between HCP Mg and MgH₂. The term $(3\bar{V}/r)\Delta\gamma_{\text{Mg} \rightarrow \text{MgH}_2}$ estimates the excess surface energy of the Mg phase that will be released upon hydriding. \bar{V} is assumed to be the average molar volume of Mg and MgH₂ (1.4×10^{-5} m³/mol and 1.8×10^{-5} m³/mol, respectively [9]), or 1.6×10^{-5} m³/mol, while an estimate of 1.76 J/m² is used for $\Delta\gamma_{\text{Mg} \rightarrow \text{MgH}_2}$ [3]. The Calphad-type thermodynamic assessment of the H-Mg-Ni ternary system is used to calculate the molar free energies of each phase in bulk form [7].

Using the above data as input for Eq. (3), the effects of particle radius on the equilibrium hydriding/dehydriding temperature are calculated for a pressure of 1×10^5 Pa (1 atm). Table 2 summarizes the experimentally determined hydride decomposition temperatures for the samples hydrided at 473 K and 573 K, T_m , along with the calculated temperatures for the reaction $\text{Mg} + \text{H}_2 \rightarrow \text{MgH}_2$, using Eq. (3) for equilibrium in a bulk samples (no surface energy effects), T_o , and the decreased temperature due to microstructural size effects, T_r , using the average crystallite sizes measured from the XRD results. Also given is the effective decrease in the enthalpy of formation, given by the last term in Eq. (3), for the measured crystallite sizes of the samples hydrided at the two temperatures. The exact behavior of the material as a function of

grain/particle size is dependent on numerous other considerations, not addressed here, but there is reasonable agreement between the measured and calculated temperatures. Decreasing grain size from 58 nm to 38 nm yields a decrease in the decomposition temperature by about 20 K, less than the 50 K observed experimentally. Never-the-less, the decrease in hydride decomposition temperature is straight-forward evidence that a nanocrystalline structure, preserved by activation at decreased temperatures, has an observable effect on the thermodynamic properties of hydrogenation in Mg-based materials.

4. Conclusions

An amorphous binary $\text{Mg}_{85}\text{Ni}_{15}$ melt-spun ribbon material was treated with an aqueous NH_4^+ solution followed by rinsing in hexanes, and by ball milling in hexanes for 30 min. Both treatments resulted in much improved activation kinetics and hydrogen storage properties when compared to the as-spun material. Activation at 473 K was possible in both the NH_4^+ -treated and ball milled samples, and required less time than for activation of the as-spun sample at 573 K. During hydriding at 573 K, the times required to fully absorb and desorb H were reduced from >800 min and 100 min, respectively, in the as-spun ribbons, to 20 min and 10 min, respectively, for the processed materials. Ball milling improved the kinetics slightly more than the NH_4^+ -treatment because of an increase in surface area. The ability to activate the material at 473 K and increased kinetics in the treated materials are a result of reduced microstructural coarsening, and the preservation of a nanocrystalline structure because of decreased exposure to high temperatures.

Thermodynamically, DSC measurements of dehydrogenation temperatures in NH_4^+ -treated samples hydride at 473 K and 573 K demonstrated that decreased crystallite size

decreases the equilibrium decomposition temperature an appreciable amount, which was confirmed with thermodynamic calculations. Because surface treatment NH_4^+ results in a lower required activation temperature, this process shows promise as an alternative method of activation and preservation of the nanocrystalline structure of Mg-based hydrogen storage materials.

Acknowledgements

EAL would like to thank the National Research Council for support under the NRC Postdoctoral Research Associateship Program.

References

1. B. Sakintuna, F. Lamari-Darkim, M. Hirscher, *Int. J. Hydrogen Energy*, **32** (2007) 1121
2. Z.X. Guo, C. Shang, K.F. Aguey-Zinsou, *J. Euro. Ceramic Soc.*, **28** (2008) 1467
3. V. Berube, G. Radtke, M. Dresselhaus, G. Chen, *Int. J. Energy Res.*, **31** (2007) 637
4. V.M. Skripnyuk, E. Rabkin, Y. Estrin, R. Lapovok, *Acta Mat.*, **52** (2004) 405
5. T. Spassov, P. Solsona, S. Surinach, M.D. Baro, *J. Alloys Comp.*, **345** (2002) 123
6. W.J. Boettinger, Y. Mishin
7. K. Zeng, T. Klassen, W. Oelerich, R. Bormann, *J. Alloys Comp.*, **283** (1999) 213
8. C.N. Singman, *J. Chem. Ed.*, **61** (1984) 137
9. "Physical Constants of Inorganic Compounds," in *CRC Handbook of Chemistry and Physics, 91st Edition*, W. M. Haynes, ed., CRC Press/Taylor and Francis, Boca Raton, FL, 2010

Table 1: Maximum capacities and required absorption/desorption times to reach 50 % and 95 % of maximum capacity at 573 K during the third cycle for the Mg₈₅Ni₁₅ ribbons in the as-spun, ball milled, and NH₄⁺-treated conditions.

	As-spun	Ball-milled	NH ₄ ⁺ -treated
Max. capacity (wt. % H)	4.6	5.4	5.2
Abs.-95 % (min)	450	22	26
Abs.-95 % (min)	22	<1	3.5
Des.-95 % (min)	53	10	20
Des.-50 % (min)	18	2	3.5

Table 2: Average crystallite sizes and measured hydride decomposition temperatures, T_m , of the NH_4^+ -treated material hydride at 473 K and 573 K. Also given are the calculated decomposition temperature for the $\text{MgH}_2 \rightarrow \text{Mg} + \text{H}_2$ reaction using the thermodynamic assessment in ref. [1], T_o , the decreased temperature due to grain size calculated using Eq. (1), T_r , and the effective decrease in the enthalpy of formation, ΔH_f .

	Hydrided @ 473 K	Hydrided @ 573 K
Crystallite Size (nm)	38±9	58±14
T_m (DSC) (K)	524	573
T_o ($\text{MgH}_2 \rightarrow \text{Mg} + \text{H}_2$) (K)	561	
T_r ($\text{MgH}_2 \rightarrow \text{Mg} + \text{H}_2$) (K)	530	551
ΔH_f (J/mol)	-2200	-1400

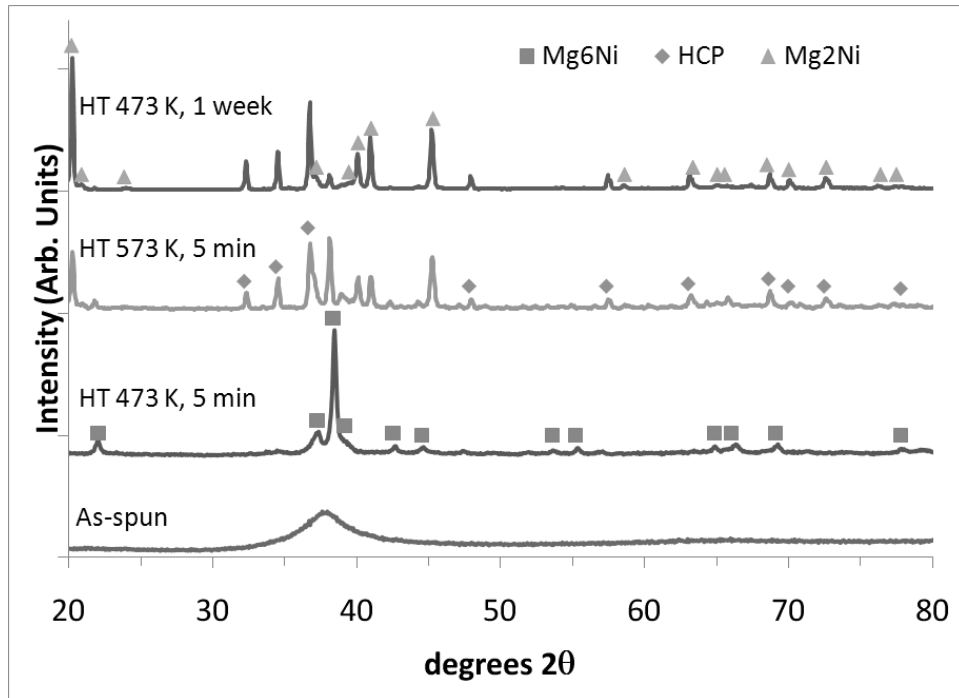


Figure 1: Activation of binary $\text{Mg}_{85}\text{Ni}_{15}$ melt-spun ribbons for the three conditions, ball milled (BM), NH_4^+ treated, and as-spun, at a temperature of *a*) 573 K, and *b*) 473K. Because the as-spun sample could not be activated at 473 K, the results at 573 K are shown for comparison in *b*.

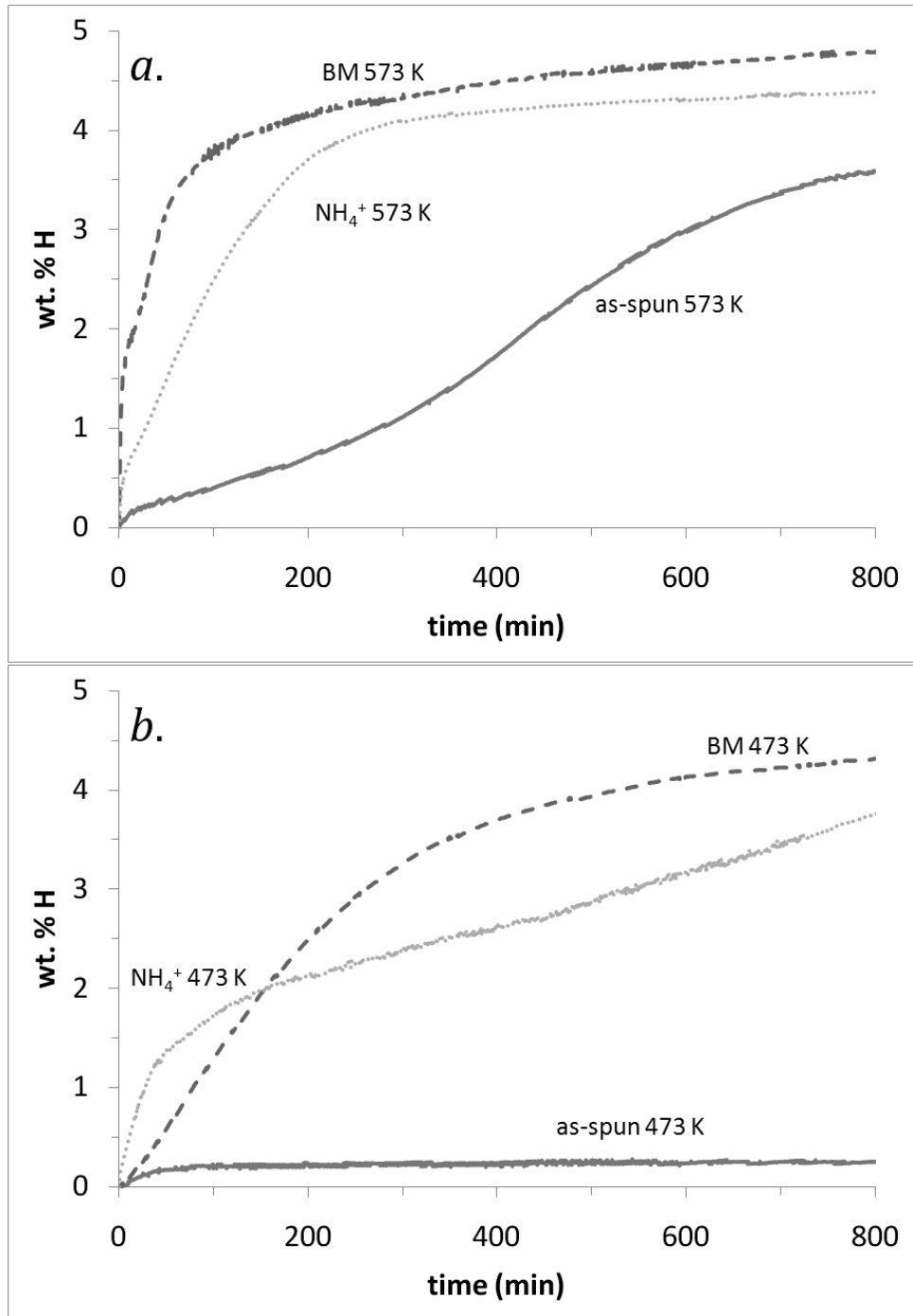


Figure 2: Activation of binary $Mg_{85}Ni_{15}$ melt-spun ribbons for the three conditions, ball milled, NH_4^+ treated, and as-spun, at a temperature of *a)* 573 K, and *b)* 473K. Because the as-spun sample could not be activated at 473 K, the results at 573 K are shown for comparison in *b.*

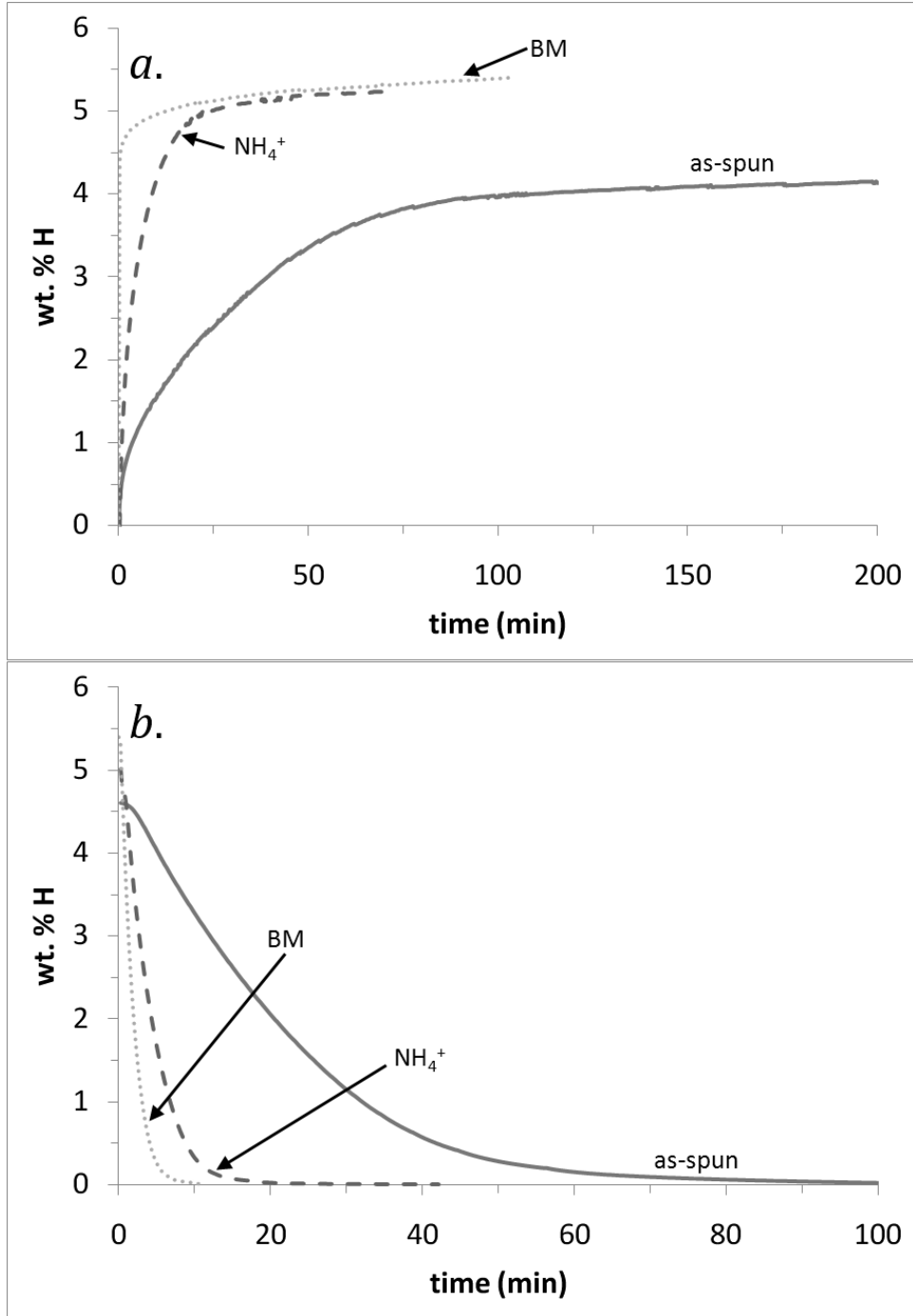


Figure 3: a) Absorption and b) desorption kinetic measurements at 573K for the binary $\text{Mg}_{85}\text{Ni}_{15}$ melt-spun ribbons in each of the three conditions, ball milled (BM), NH_4^+ treated, and as-spun. The as-spun material was activated at 573 K while the ball milled and NH_4^+ -treated samples were activated at 473 K.

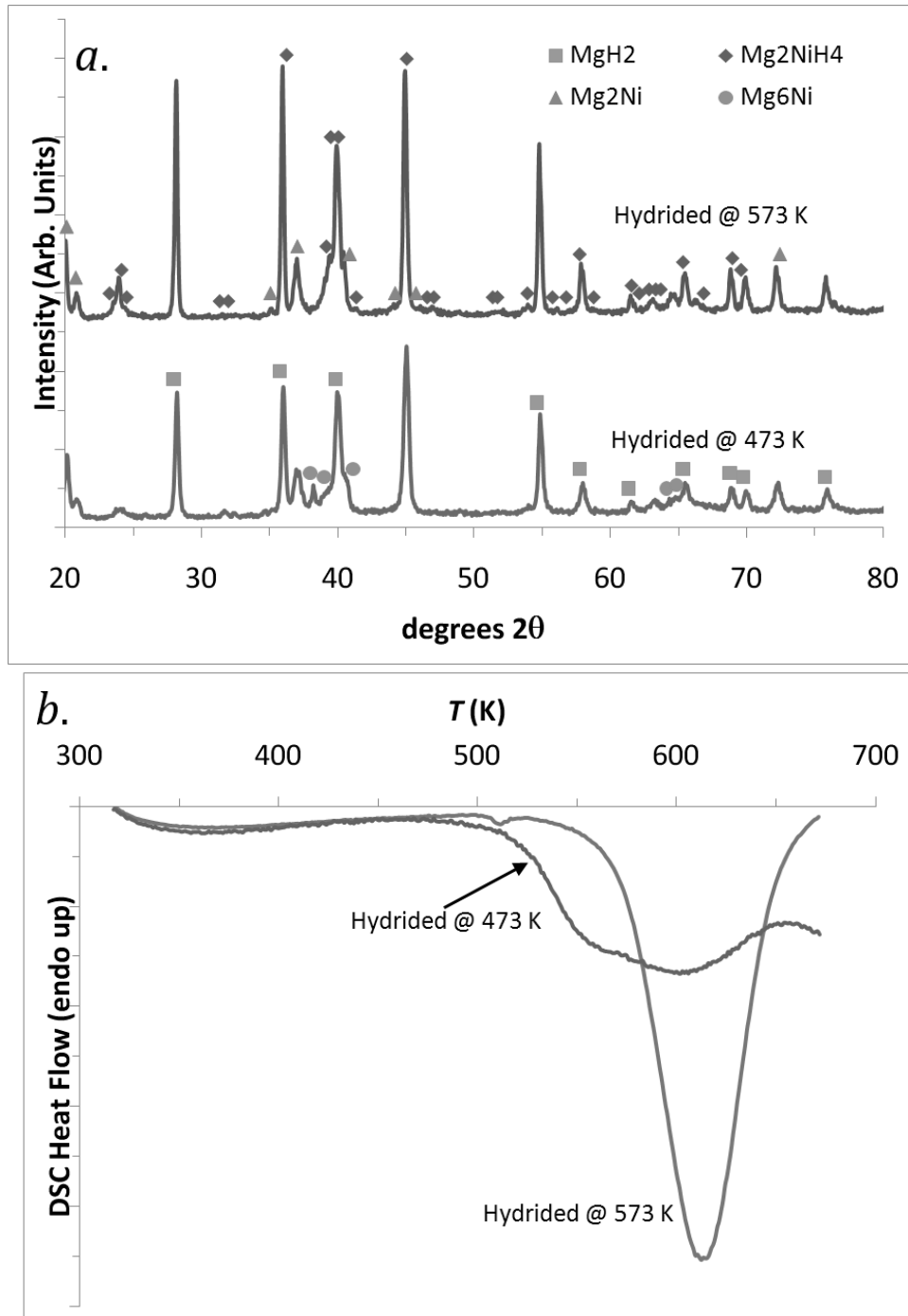


Figure 4: a) XRD patterns for the NH_4^+ treated alloy hydrided at 473 K and 573 K. Some Mg_2Ni and Mg_6Ni remain in the material due to incomplete hydriding. b) DSC scans for the NH_4^+ treated alloy hydrided at 473 K and 573 K showing a decrease in the onset of dehydration for the alloy hydrided at 473 K.